

Realization and modeling of rf superconducting quantum interference device meta-atoms

M. Trepanier,^{1,*} Daimeng Zhang,^{2,†} Steven M. Anlage,^{1,2} and Oleg Mukhanov³

¹*Department of Physics, CNAM, University of Maryland, College Park, Maryland 20742-4111, USA*

²*Department of Electrical and Computer Engineering,*

University of Maryland, College Park, Maryland 20742-3285, USA

³*Hypres, Inc., 175 Clearbrook Road, Elmsford, New York 10523, USA*

(Dated: June 6, 2019)

We have prepared meta-atoms based on radio frequency superconducting quantum interference devices (RF SQUIDS) and examined their tunability with dc magnetic field, rf current, and temperature. The RF SQUIDS are superconducting split ring resonators in which the usual capacitance is supplemented with a Josephson junction. The dc and ac Josephson effects introduce strong nonlinearity in the rf properties of the meta-atom, and these are modeled with the resistively and capacitively-shunted junction model. We find excellent agreement between the data and the model for the tunable properties of the RF SQUID meta-atoms. A magnetic field tunability of 80 THz/Gauss at 12 GHz is observed, a total tunability of 56% is achieved, and a unique electromagnetically-induced transparency feature at intermediate excitation powers is demonstrated for the first time.

I. INTRODUCTION

Metamaterials are artificially structured media that are designed to have unique electromagnetic properties which are not ordinarily found in nature. These properties arise from both the structure of individual meta-atoms and the interactions between these elements, resulting in interesting collective behavior. A wide variety of properties and applications have been pursued using metamaterials, including negative index of refraction [1] [2] [3], super-resolution imaging [4] [5], cloaking [6] [7], transformation optics [8] [9], and perfect absorption [10].

Most of the applications invoking novel optical properties impose three stringent constraints on the metamaterials. First, the metamaterial must have a low attenuation for the electromagnetic waves passing through it. Features such as evanescent wave amplification [11] and negative refraction are strongly suppressed with even small amounts of loss [12] [13] [14] [15] [11] [16]. For example, the enhanced loss in metamaterials approaching the plasmonic limit has imposed a severe limitation on visible wavelength metamaterials composed of noble metal meta-atoms [17] [18] [19] [20]. Secondly, the meta-atoms must be of deep sub-wavelength dimensions so that the electromagnetic properties can be interpreted as those of an effective medium, i.e. to achieve the metamaterial limit, as opposed to the photonic crystal limit. This has been an issue both in the visible and in the microwave regime, where meta-atom sizes often approach the scale of the wavelength in size to minimize losses [21] [22]. Thirdly, it is desirable to make metamaterials that have textured properties in space (e.g. for cloaking or transformation optics), or that can be tuned and

re-configured after the metamaterial has been fabricated [23]. Being able to tune the electromagnetic response over a wide range, and on short time scales, is highly desirable for applications such as software-defined radio [24] and filters for digital rf receivers [25].

Superconducting metamaterials have been proposed to address all three of the major constraints mentioned above [26]. In addition, the quantum coherent nature of the superconducting state leads to qualitatively new phenomena such as fluxoid quantization and Josephson effects, which can significantly expand the number of new electromagnetic properties not found in nature. Here we focus on the tunability and reconfigurable nature of superconducting Josephson metamaterials.

Superconductors are fundamentally nonlinear electromagnetic entities. All superconductors are endowed with an intrinsic nonlinearity known as the nonlinear Meissner effect [27] [28]. The Meissner effect is the spontaneous exclusion of magnetic flux from the bulk of an object when it undergoes the normal to superconducting phase transition, even in a static magnetic field [29]. The material will achieve a lower free energy by entering the superconducting state (with a non-zero superconducting order parameter Ψ and superfluid density $\sim |\Psi|^2$) and generating dissipationless screening currents to exclude the field, as long as the field is not too great. However, as the magnitude of the field is increased the superconductor must generate stronger screening currents (requiring a greater kinetic energy), resulting in a suppression of the superconducting order parameter, and the superfluid density. As a consequence, the superfluid plasma frequency [30] is decreased, and the magnetic screening length is enhanced. This in turn gives rise to an increase in inductance of any current-carrying circuit element made up of the superconductor, thereby generating a nonlinear electromagnetic response [31] [32]. In general this intrinsic nonlinearity will be encountered when superconductors are pushed toward the limits of their existence in param-

* mctrep@umd.edu; these authors contributed equally

† dmchang@umd.edu; these authors contributed equally

eter space. This space is spanned by three quantities: temperature, applied magnetic field, and applied current. The limits of superconductivity are T_c (the critical temperature), B_c or B_{c2} (the thermodynamic critical field or upper critical field), and J_c (the critical current density). As superconductors are pushed towards these limits, the nonlinear properties will be strongly enhanced.

Early on it was found that superconducting metamaterials are tunable with temperature due to the temperature dependence of the superfluid density and kinetic inductance [33] [34]. This type of tunability has been exploited in a variety of superconducting metamaterials with some success [35] [36] [37] [38] [39]. However, temperature tuning is generally considered to be too slow due to the fact that thermal inertia of the meta-atoms can be large, even at low temperatures. Typical estimates for temperature tuning response times are on the order of $10\mu\text{s}$ [40].

It is also possible to tune the properties of superconducting metamaterials with an applied current. Currents can be used to directly cause superfluid de-pairing, resulting in an increase of kinetic inductance of the superconductor [41]. For example, a tunable amplitude modulator has made use of transport currents applied through superconducting Nb wiring making up the metamaterial to vary the attenuation of the medium for sub-THz radiation [40]. However, applied currents often induce magnetic vortices in the superconducting material before the de-pairing critical current is reached [42] [40]. These vortices move under the influence of the high-frequency currents, creating enhanced dissipation, in addition to enhanced inductance. In general the additional dissipation renders the superconductors less attractive for applications.

Magnetic field tuning of superconductors is attractive for applications because it can be accomplished quickly, and it can have a large effect on the electrodynamic properties of the metamaterial. Both DC and RF magnetic fields have been employed to tune the properties of superconducting split-ring resonators (SRRs) [43] [44]. A DC magnetic field was shown to add magnetic flux to a thin film Nb SRR, increasing its inductance and loss [43]. The RF magnetic field created enhanced RF screening currents at discrete locations in the SRR, eventually resulting in enhanced inductance and dissipation as magnetic flux moved into and out of the superconducting film at high frequency [43] [45] [46] [47] [48] [49]. It was also found that a superconducting resonator exhibiting an analog of electromagnetically-induced transparency showed a strong switching behavior at high excitation power [39], for similar reasons. However, the insertion of magnetic flux into superconducting materials is often too slow and too dissipative to be used for tuning applications. It would be better to employ a low-dissipation quantum effect to tune superconducting meta-atoms. For example, the use of flux quantization to discretely tune a superconducting meta-atom has been proposed [50].

A. Superconducting Meta-Atoms Employing the Josephson Effect

The addition of the Josephson effect to superconducting metamaterials adds a mechanism of tunability that offers high speed, a large degree of tunability, and low dissipation. Under certain circumstances a superconductor can be described by a macroscopic phase-coherent complex quantum wavefunction $\Psi = \sqrt{n_s}e^{i\theta}$ [29]. This wavefunction inherits its phase coherence from the underlying microscopic BCS wavefunction describing the Cooper pairing of all electrons in the metal. The absolute square of the macroscopic quantum wavefunction is interpreted as the local superfluid density $n_s \sim |\Psi|^2$ [51]. When two superconductors are brought close together and separated by a thin insulating barrier, there can be quantum mechanical tunneling of Cooper pairs between the two materials [52] [29]. This tunneling results in two types of Josephson effect. The first produces a DC current between the two superconductors which depends on the gauge-invariant phase difference between their macroscopic quantum wavefunctions as $I = I_c \sin \delta(t)$, where $\delta(t) = \theta_1(t) - \theta_2(t) - \frac{2\pi}{\Phi_0} \int_1^2 \vec{A}(\vec{r}, t) \cdot d\vec{l}$ is the gauge-invariant phase difference between superconductors 1 and 2, $\vec{A}(\vec{r}, t)$ is the vector potential in the tunneling region between the superconductors, arising from magnetic fields, I_c is the critical (maximum) current of the junction, and $\Phi_0 = \frac{h}{2e} \cong 2.07 \times 10^{-15} \text{Tm}^2$ is the flux quantum (h is Planck's constant and e is the electronic charge). The DC Josephson effect states that a DC current will flow between two superconductors connected by a tunnel barrier, in the absence of a DC voltage, and the magnitude and direction of that current depend on a nonlinear function of the phase differences of their macroscopic quantum wavefunctions, as well as applied magnetic field.

The AC Josephson effect relates a DC voltage drop on the junction to a time-varying gauge-invariant phase difference, and therefore to an AC current in the junction: $\frac{d\delta}{dt} = \frac{2\pi}{\Phi_0} V$, where V is the DC voltage across the tunnel barrier. The AC impedance of a Josephson junction contains both resistive and reactive components in general [53]. At low frequencies and currents, the impedance of a Josephson junction can be treated with the resistively and capacitively shunted junction (RCSJ) model [51]. In the presence of both DC and AC applied currents in the junction, the nonlinear inductance of the junction can be described approximately as [51]

$$L_{JJ} = \frac{\Phi_0}{2\pi I_c \cos \delta}. \quad (1)$$

The Josephson inductance is a strong function of applied currents and fields. Tuning of Josephson inductance in a transmission line metamaterial geometry was considered theoretically by Salehi [54] [55].

In this work we focus on a meta-atom made up of a single Josephson junction in a superconducting loop, commonly known as a radio frequency superconducting quantum interference device (RF SQUID). An RF SQUID

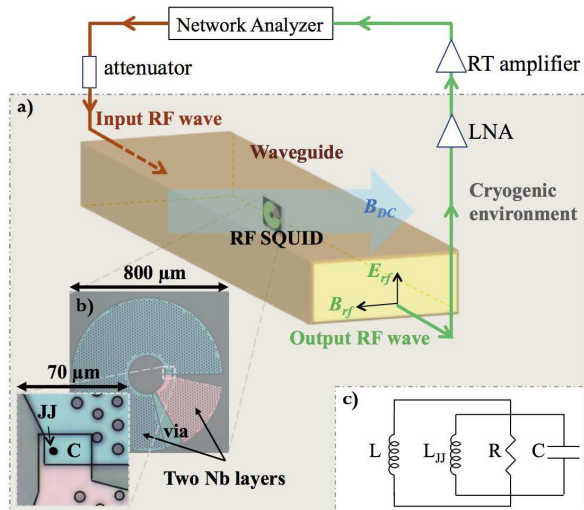


FIG. 1. a) Schematic diagram of the experiment showing the flow of the rf signal from the network analyzer (at room temperature, RT), through the attenuator, into waveguide (in the cryogenic environment), through the RF SQUID sample biased by DC magnetic field, out of the waveguide through a series of amplifiers, and back to the network analyzer. b) Micrograph of an RF SQUID meta-atom, consisting of two perforated Nb layers connected by a via and Josephson junction (JJ) which is $2.6 \mu\text{m}$ in diameter. The overlap capacitance is the small rectangular region immediately surrounding the junction ($600 \mu\text{m}^2$). c) Circuit diagram of the RF SQUID modeled as an RCSJ in parallel with loop inductance L

meta-atom is shown in Fig. 1(b); it is a natural quantum analog of the split ring resonator. As such, we shall examine the electromagnetic properties of the SQUID near its self-resonant frequency. The original purpose of the RF SQUID was to measure small magnetic fields and operate as a flux to frequency transducer [56] [57]. The first proposal to use an array of RF SQUIDs as a metamaterial was made by Du, Chen and Li [58] [59]. Their calculation assumes the SQUID has quantized energy levels and considers the interaction of individual microwave photons with the lowest lying states of the SQUID potential. For small detuning of the microwave photon frequency above the transition from the ground state to the first excited state, the medium will present a negative effective permeability. However, the frequency region of negative permeability is diminished by a non-zero de-phasing rate, and negative permeability will disappear for de-phasing rates larger than a critical value.

A treatment of RF SQUIDs interacting with classical electromagnetic fields was presented by Lazarides and Tsonis [60]. They considered a two-dimensional array of RF SQUIDs in which the Josephson junction was treated as a parallel combination of resistance, capacitance, and Josephson inductance. Near resonance, a single RF SQUID can have a large diamagnetic response. For an array, there is a frequency and RF-magnetic field region in which the system displays a negative real part of effective permeability. The permeability is in fact

oscillatory as a function of applied magnetic flux, and will be suppressed with applied fields that induce currents in the SQUID that exceed the critical current of the Josephson junction. Similar calculations that included interactions between the RF SQUIDs were carried out by Maimistov and Gabitov [61]. Related work on a one-dimensional array of superconducting islands that can act as quantum bits (qubits) was considered by Rakhmanov, et al. [62]. When interacting with classical electromagnetic radiation, the array can create a quantum photonic crystal that can support a variety of nonlinear wave excitations. A similar idea based on a SQUID transmission line was implemented to perform parametric amplification of microwave signals [63] [64]. A dc-field tunable one-dimensional SQUID metamaterial embedded in a co-planar waveguide structure has been recently demonstrated [65].

Our objective in this paper is to demonstrate the first SQUID metamaterial in a geometry that can be easily extended to a fully three-dimensional structure where they can interact with free-space electromagnetic waves. We demonstrate that the RF SQUID meta-atoms are remarkably tunable with very small DC magnetic fields, as well as temperature and RF currents. The rest of the paper is organized as follows. We first present several models of RF SQUID linear and nonlinear behavior, then discuss the details of their design and fabrication. Section V presents our experimental results of the RF SQUID meta-atoms in waveguide geometries, demonstrating tunability of the meta-atom properties with DC flux, temperature, and RF flux. Section VI is a comparison of data and model predictions, and discussion of the results, and Section VII serves as a conclusion.

II. MODELING

An ideal Josephson junction can be treated as an inductor with a variable inductance controlled by the gauge-invariant phase difference as given by Eq. 1. A more realistic model shunts the junction with a sub-gap resistance R (representing the tunneling of normal state electrons across the junction) and capacitance C (the capacitance of two overlapping conductors separated by an insulator). We model the RF SQUID as a resistively and capacitively shunted junction (RCSJ) in parallel with an inductor which represents the inductance, L , of the superconducting loop. The result is an RLC circuit (see circuit diagram in Fig. 1(c)) with a resonant frequency given by

$$f_0(T, \Phi_{app}) = \frac{1}{2\pi \sqrt{\left(\frac{1}{L} + \frac{1}{L_{JJ}(T, \Phi_{app})}\right)^{-1} C}}. \quad (2)$$

To understand the behavior of the resonance as a function of temperature, T , and applied flux, Φ_{app} , it is necessary to solve for $\delta(T, \Phi_{app})$ and find L_{JJ} .

We use the RCSJ model to solve for the gauge-invariant phase difference δ subject to the condition that the total flux through the loop must be an integer number (n) of flux quanta, i.e. $\Phi = n\Phi_0$. The total flux is related to the applied flux and the current-induced flux by

$$\Phi_{app} = \Phi + LI \quad (3)$$

where $\Phi_{app} = \Phi_{DC} + \Phi_{rf} \sin \omega t$, $\Phi = \frac{\Phi_0 \delta}{2\pi}$ is the total flux through the loop, and I is the current through the loop, which is the sum of the currents through the junction, the resistor, and the capacitor. We have taken $n = 1$ because the choice of integer just shifts δ (which has 2π periodicity) by 2π . We can rewrite Eq. 3 in the terms of the gauge-invariant phase difference of the junction, δ , as

$$\begin{aligned} \Phi_{DC} + \Phi_{rf} \sin \omega t &= \frac{\Phi_0 \delta}{2\pi} + \\ L \left(I_c \sin \delta + \frac{1}{R} \frac{\Phi_0}{2\pi} \frac{d\delta}{dt} + C \frac{\Phi_0}{2\pi} \frac{d^2\delta}{dt^2} \right) \end{aligned} \quad (4)$$

which can be recast in non-dimensional form as

$$\begin{aligned} 2\pi [f_{DC} + f_{rf} \sin \Omega\tau] &= \\ \delta + \beta_{rf} \sin \delta + \frac{1}{Q} \frac{d\delta}{d\tau} + \frac{d^2\delta}{d\tau^2} \end{aligned} \quad (5)$$

where $\omega_{0,geo} = \sqrt{\frac{1}{LC}}$, $\tau = \omega_{0,geo} t$, $\Omega = \frac{\omega}{\omega_{0,geo}}$, $\beta_{rf} = \frac{2\pi LI_c}{\Phi_0}$, $Q = R\sqrt{\frac{C}{L}}$, $f_{rf} = \frac{\Phi_{rf}}{\Phi_0}$, and $f_{DC} = \frac{\Phi_{DC}}{\Phi_0}$.

A well-studied mechanical analogue of the Josephson junction is the driven and damped pendulum [66]. Equation 5 resembles the nonlinear differential equation that governs that system. However, incorporating the junction into a superconducting loop subject to flux quantization introduces an additional linear term. Unlike the driven, damped pendulum, this equation is linear in the high power limit in addition to the low power limit. For our chosen parameters, δ is always periodic in time and its variation is dominated by the same frequency as the driving flux. We do not observe chaos for parameter values relevant to the experiment.

At intermediate powers the full non-linear Eq. 5 must be solved for δ , and therefore $f_0(T, f_{DC}, f_{rf})$, but the equation can be linearized and simplified in the low and high power limits. In the low rf power limit (where it is assumed that the time-varying component of the gauge invariant phase difference is very small i.e. $\delta_{rf}(\tau) \ll 1$) Eq. 5 can be linearized by separating the phase difference into a DC and rf components, i.e.

$$\delta = \delta_{DC} + \delta_{rf}(\tau). \quad (6)$$

Equation 5 simplifies to the following time-independent and time-dependent equations:

$$2\pi f_{DC} = \delta_{DC} + \beta_{rf} \sin \delta_{DC} \quad (7)$$

$$2\pi f_{rf} \sin \Omega\tau = \alpha \delta_{rf} + \frac{1}{Q} \frac{d\delta_{rf}}{d\tau} + \frac{d^2\delta_{rf}}{d\tau^2} \quad (8)$$

where $\alpha = 1 + \beta_{rf} \cos \delta_{DC}$. In this case the DC flux dictates δ_{DC} and Eq. 8 has an analytic solution for δ_{rf} given by

$$\delta_{rf} = 2\pi f_{rf} \frac{(\alpha - \Omega^2) \sin \Omega\tau - (\Omega/Q) \cos \Omega\tau}{(\alpha - \Omega^2)^2 + (\Omega/Q)^2}. \quad (9)$$

From this result one finds that δ and consequently $f_0(T, f_{DC})$ are periodic functions of f_{DC} with maximum and minimum values at $f_{DC} = n$, and $f_{DC} = n + 1/2$ respectively, where n is any integer.

The resonant frequency of the SQUID, f_0 , is also temperature dependent as a result of the temperature dependence of the critical current, I_c . As temperature increases the maximum frequency decreases and the minimum frequency increases resulting in a reduction of total flux tunability of the SQUID. When the temperature reaches the critical temperature of niobium (9.2 K), $|L_{JJ}|$ is expected to diverge (since $I_c \rightarrow 0$). In this case the Josephson junction loses the ability to modify the resonance and the resonant frequency reduces to

$$f_{0,geo} = \frac{1}{2\pi\sqrt{LC}}. \quad (10)$$

This resonance depends solely on the non-junction properties of the SQUID and is insensitive to applied flux, Φ_{app} , and temperature, T .

Also note that Eq. 5 is linear in the high power limit (where it is assumed $\delta_{rf} \gg 1$ since $\sin \delta + \delta \approx \delta$), where it separates into the following time dependent and time independent equations:

$$2\pi f_{DC} = \delta_{DC} \quad (11)$$

$$2\pi f_{rf} \sin(\Omega\tau) = \delta_{rf} + \frac{1}{Q} \frac{d\delta_{rf}}{d\tau} + \frac{d^2\delta_{rf}}{d\tau^2} \quad (12)$$

Equation 12 has the same analytic solution as Eq. 9 with α replaced by 1, so unlike Eq. 9 it has no dependence on temperature or DC flux. In the high power limit the Josephson junction no longer plays a role and the resonant frequency reduces to the same value as in the high temperature limit, Eq. 10. As in the high temperature limit, the SQUID is insensitive to applied flux and temperature.

III. DESIGN AND FABRICATION

The RF SQUID meta-atoms were manufactured using the Hypres 0.3 $\mu\text{A}/\mu\text{m}^2$ Nb/AlO_x/Nb process on silicon substrates. However, measurements of other junctions from this run suggest the critical current density is actually closer to 0.2 $\mu\text{A}/\mu\text{m}^2$ at 4.2 K. The superconducting loop is composed of two Nb films (135 nm and 300 nm thick) which are connected by a via and a Nb/AlO_x/Nb Josephson junction (see Fig. 1(b)). There is additional capacitance where these layers overlap (with

SiO₂ dielectric) which is necessary to bring the resonant frequency within the measurable range. When designing the SQUIDs we have control over the inner and outer radius of the loop and thus the loop inductance L , the critical current of the junction I_c , and the overlap capacitance C .

Values for L , I_c , and C were chosen to maximize tunability within the measurable frequency range 6.5-22 GHz (dictated by the available waveguides) while remaining in the low noise ($\Gamma = \frac{2\pi k_B T}{\Phi_0 I_c} < 1$ and $L_F = \frac{1}{k_B T} \left(\frac{\Phi_0}{2\pi}\right)^2 \gg L$ [67]) and non-hysteretic ($\beta_{rf} = \frac{2\pi L I_c}{\Phi_0} < 1$) limits. The inner and outer radii of the SQUID loop are 100 μm and 400 μm respectively with 3 μm diameter holes in the film every 10 μm to pin vortices [68]. We estimate L to be 0.33 nH based on FastHenry calculations [69]. The area of the Josephson junction and the area of the capacitor are 5.3 μm^2 and 600 μm^2 respectively, yielding nominal design values of $I_c(4.2 \text{ K}) = 0.97 \mu\text{A}$ and $C = 0.32 \text{ pF}$.

IV. EXPERIMENT

The RF SQUID is orientated in a 7.6 cm long Ku rectangular waveguide (single propagating mode operating frequency range from 9.5-19 GHz) as shown in Fig. 1(a). An attenuated microwave signal from an Agilent E8364C network analyzer excites a TE₁₀ mode in the waveguide producing an rf magnetic field, B_{rf} , primarily perpendicular to the plane of the SQUID. The transmission, S_{21} , is measured after a cryogenic low noise amplifier (LNA) and a room-temperature (RT) amplifier. The experiment is conducted in a three-stage pulsed-tube cryostat with a sample base temperature of 6.5 K. The sample is magnetically shielded by a mu-metal cylinder and a superconducting niobium open cylinder inside the cryostat. Superconducting coils surrounding the waveguide bias the SQUID by generating a perpendicular DC magnetic field, B_{DC} in the range from 0 to 1 μT .

Our experiment detects the resonance as a dip in the frequency dependent transmission magnitude through the waveguide $|S_{21}(\omega)|$. We have considered two methods for calculating scattering parameters from the solution for δ . One method is to consider the SQUID an effective medium with an effective relative permeability, μ_r [70] [65],

$$\mu_r = 1 + F \left(\left\langle \frac{\Phi_{ac}}{\Phi_{rf} \sin \omega t} \right\rangle - 1 \right), \quad (13)$$

where Φ_{ac} is the AC flux response of the loop, the angle brackets represent time averaging, and F is the filling fraction of the SQUID in the medium [60] [59]. S_{21} is proportional to the ratio of the transmitted electric field, E_T , to the incident field E_0 , and can be calculated using the continuity of E and H fields at the boundaries of the

effective medium and the empty waveguide as

$$S_{21} = \sqrt{\gamma} \frac{E_T}{E_0} = \frac{\sqrt{\gamma}}{\cos kl - \frac{i}{2} \left(\frac{1}{\gamma} + \gamma \right) \sin kl}, \quad (14)$$

where l is the length of the medium, $\gamma = \frac{k}{\mu_r k_0}$, $k = \sqrt{\mu_r \left(\frac{\omega}{c}\right)^2 - \left(\frac{\pi}{a}\right)^2}$ is the wave number in the medium, and $k_0 = k(\mu_r = 1)$ is the wave number in the empty waveguide. Since we are working with a single SQUID (as opposed to an array) the choice of l and F is not straightforward. We use them as fitting parameters (along with R) to match the model with the width and depth of the measured resonances. What is important to the fit is the relationship between F and l , which we find to be $F = \frac{A_{loop}}{0.79l}$, where A_{loop} is the area of the SQUID loop (calculated from the average radius of the SQUID).

An alternate method of estimating S_{21} is based on calculating the power dissipated in the resistor, R in Fig. 1(c).

$$S_{21} = \sqrt{\frac{P_T}{P_0}} = \sqrt{1 - \frac{V^2}{RP_0}} \quad (15)$$

where P_T is the transmitted power and P_0 is the incident power. This assumes that the only power not transmitted through the waveguide is the power dissipated in the resistor. It does not account for reflection or other loss mechanisms.

V. RESULTS

When cooled below the transition temperature of Nb, the RF SQUID meta-atom shows a resonant response in $S_{21}(\omega)$ within the designed frequency range. The RF SQUID meta-atom resonance responds to three different tuning parameters: DC magnetic field, temperature, and rf power. Modifying the resonant frequency by DC magnetic field is the most straightforward. Figure 2 shows the experimental results for $|S_{21}|$ of an RF SQUID meta-atom as a function of DC flux and frequency. The incident rf power at the sample and the temperature were fixed at -80 dBm and 6.5 K, respectively. Resonance dips in $|S_{21}(\omega)|$ appear as the red features in the plot against a yellow background of unaffected signals ($|S_{21}| = 0\text{dB}$). The signal was extracted by subtracting $|S_{21}|$ at 16 K (which is well above the critical temperature) from $|S_{21}|$ at 6.5 K, removing a background variation, and applying a threshold to identify the resonance. The transmission dips show good periodicity as a function of DC flux, with a maximum resonant frequency $16.9 \pm 0.3 \text{ GHz}$ and minimum at or below 10 GHz. The cutoff frequency of the Ku waveguide is 9.5 GHz which imposes a lower frequency limit on this measurement; when the same sample is measured in an X band waveguide (single propagating mode operating frequency range from 6.6-13 GHz) the lowest resonant frequency is found to be $9.5 \pm 0.5 \text{ GHz}$.

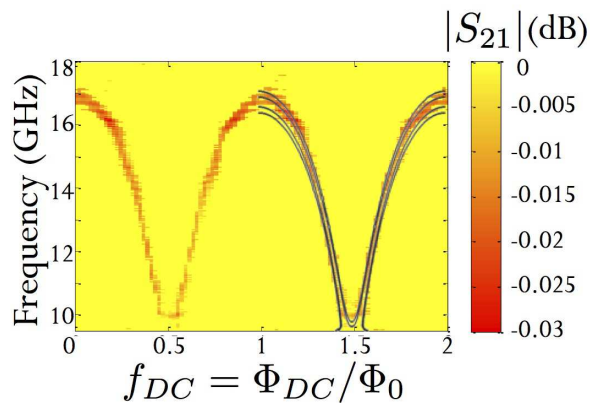


FIG. 2. Experimental measurements of $|S_{21}|$ of the RF SQUID meta-atom as a function of frequency and applied DC flux at -80 dBm rf power and 6.5 K. The resonant response is identified by the red features. There are contour lines for $|S_{21}|$ at -0.005 and -0.01 dB generated by the model, Eq. 14.

At an rf power of -80 dBm, ($\Phi_{rf} \approx 0.003\Phi_0$) the low power linearized equation (Eq. 8) is valid (since $\delta_{rf} \ll 1$). We treat the RF SQUID as an effective medium in the waveguide and the contour lines of $|S_{21}(\omega, \Phi_{DC})|$ calculated from Eqs. 7, 9, 13, and 14 are plotted with the experimental data in Fig. 2. There is good agreement with experimental data both in terms of flux dependence and magnitude of the tunability (~ 7 GHz), and magnitude of the resonance dip in $|S_{21}(\omega)|$. The capacitance C and critical current $I_c(6.5 \text{ K})$ are adjusted from their nominal values and taken to be 0.42 pF and 0.55 μA , respectively. These values were chosen so the resonant frequency at $T = 6.5 \text{ K}$ and $\Phi_{DC} = 0$ match the experimental results in both the low and high power limits i.e. $f_0(6.5 \text{ K}, \Phi_{DC} = 0) = 16.8 \text{ GHz}$ for low power (Eq. 2) and $f_{0,geo} = 13.5 \text{ GHz}$ (Eq. 10) for high power.

As the temperature changes, the DC flux tunability of ~ 7 GHz at 6.5 K is modified. The red features in Fig. 3 show the DC flux tuned resonances at 6.5 K, 7.6 K, and 8.3 K for an rf power of -80 dBm. The increased temperature reduces the flux tunability from ~ 7 GHz at 6.5 K, to ~ 3 GHz at 7.6 K, and ~ 1 GHz at 8.3 K. The grey lines follow the resonance dips by using the solution for δ_{DC} from Eq. 7 and calculating the resonant frequency using Eqs. 1 and 2 (assuming $\delta \approx \delta_{DC}$). The only parameter varied to fit this data is the temperature dependent critical current of the junction. We also performed a series of low power measurements of $|S_{21}|$ as a function of frequency and dc flux for various fixed temperatures ranging from 6.5 to 9.2 K and observed that at $f_{DC} = 0$ the resonant frequency decreases from 17 to 13.5 GHz with increasing temperature and when $f_{DC} = 1/2$ the resonant frequency increases from 9.5 to 13.5 GHz over the same temperature range. The reduction in tunability with increased temperature is consistent with the predictions of the model as discussed in Sec. II. Also consistent with the model, the resonant frequency saturates

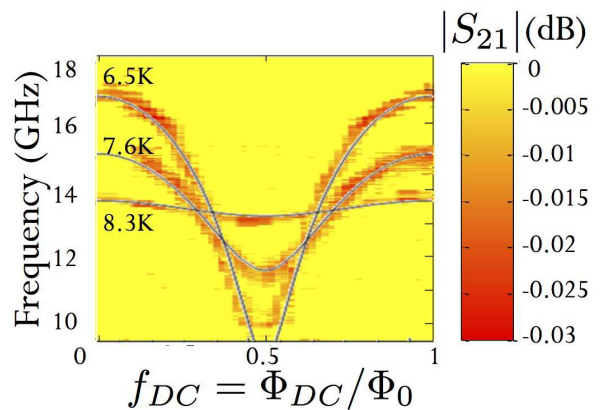


FIG. 3. Experimental measurements of $|S_{21}|$ of the RF SQUID meta-atom as a function of frequency and applied DC flux at three different temperatures, 6.5 K, 7.6 K, and 8.3 K, and -80 dBm rf power. The resonant response is identified by the red features. The solid lines are the resonant frequency calculated by Eqs. 1, 2, and 7.

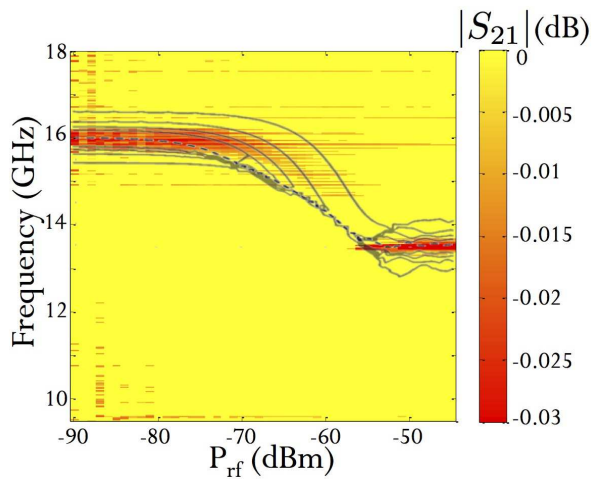


FIG. 4. Experimental measurements of $|S_{21}|$ of the SQUID meta-atom as a function of frequency and rf power at fixed DC flux, $f_{DC} = 1/6$ and temperature $T = 6.5 \text{ K}$. The resonant response is identified by the red features. The contour lines for $|S_{21}|$ at -0.04, -0.03, -0.02, and -0.01 dB are generated by the model, Eq. 15. The dashed line indicates the model-determined resonant frequency (minimum of $|S_{21}(\omega)|$).

in the high temperature limit at $f_{0,geo} = 13.5 \pm 0.2 \text{ GHz}$ (Eq. 10).

As discussed previously, the properties of a superconducting metamaterial can be modified by current, or in this case, the current induced in the meta-atom by Φ_{rf} . Figure 4 shows the experimental values of $|S_{21}|$ as a function of rf power and frequency for a representative case of $f_{DC} = 1/6$ and $T = 6.5 \text{ K}$. The resonant response is indicated by the red features. When the rf power is low, the resonance remains at a fixed value, 16 GHz, and the resonance dip has a constant depth. As the rf power increases, the resonant frequency decreases and the reso-

nance dip becomes shallower. The resonance disappears at intermediate powers before reappearing as a strong resonance at high power (-55 dBm).

Calculating the rf power dependence of the resonance requires a full numerical solution of the nonlinear Eq. 5. Instead of regarding the RF SQUID as an effective medium, we employ Eq. 15 to estimate $|S_{21}|$. The results of this calculation are plotted as contour lines in Fig. 4 and the calculated minimum of $|S_{21}|$ is plotted as a dashed line. Both show excellent agreement with the experimental results, including the depth of the $|S_{21}|$ dip, the frequency at which the SQUID properties reach high-power saturation, and the disappearance of the resonance dip at intermediate rf powers.

There are two transition points in the observed rf power dependent resonance at ≈ -75 dBm ($\Phi_{rf} \approx 0.006\Phi_0$) and -57 dBm ($\Phi_{rf} \approx 0.05\Phi_0$). We can understand the significance of these powers and the behavior in the low, intermediate, and high power regions using the model discussed in Sec. II. In the low power limit, the resonance response does not change with increasing rf power because S_{21} from Eq. 15 does not depend on input rf power, P_0 , since $P_0 \propto V^2$ ($V \propto f_{rf}$ from Eq. 9 and $f_{rf} \propto \sqrt{P_0}$ because of the relationship between input power and magnetic fields in a waveguide).

The first transition occurs at an rf power of ≈ -75 dBm, where the resonance begins to shift to lower frequencies and the resonance dip becomes shallower. This rf power corresponds to where the oscillation amplitude of δ during an rf period is $\pi/2$ at resonance. The resonant frequency is modified because above -75 dBm rf power, the time averaged phase difference $\langle \delta \rangle$ deviates from δ_{DC} . In the case of $f_{DC} = 1/6$, $\langle \delta \rangle > \delta_{DC}$ resulting in a decrease in $\cos \delta$ from its low power value, a corresponding increase in L_{JJ} (Eq. 1), and an ultimate decrease in resonant frequency f_0 (Eq. 2). However in the case of $f_{DC} = 1/2$, the modification in $\langle \delta \rangle$ causes an increase in $\cos \delta$ from its low power value and an ultimate increase in resonant frequency, f_0 . This is consistent with the experimental results. The resonance dip becomes shallower because V is no longer proportion to f_{rf} ; instead the input power, P_0 , increases more than the dissipated power, V^2/R .

The second transition occurs at an rf power of -57 dBm where δ oscillates with an amplitude exceeding 2π on resonance and the Josephson junction undergoes multiple phase slips each rf period. At this power we can utilize the high rf power limit (Eq. 12), where the tunable resonant frequency reduces to the same fixed value as the high temperature limit (Eq. 10), namely $f_{0,geo} = 13.5$ GHz. We expect the losses to be greater in this regime because the phase slips are dissipative, resulting in a deeper $|S_{21}(\omega)|$ resonance dip, which is reflected in the data.

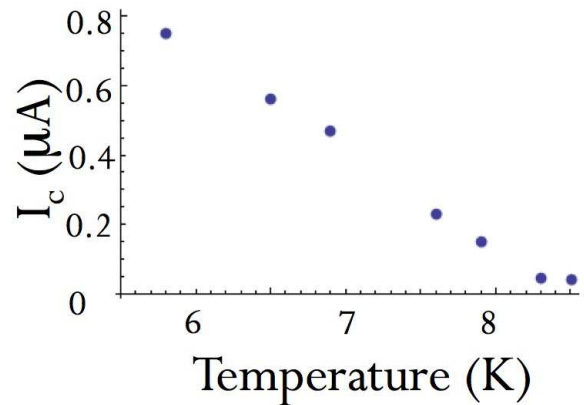


FIG. 5. Critical current temperature dependence $I_c(T)$ determined from measured maximum resonant frequencies as a function of DC flux at corresponding fixed temperatures

VI. DISCUSSION

The key parameters governing the properties of the SQUID meta-atom are the critical current $I_c(T)$, the capacitance C , the sub-gap resistance R , and the loop inductance L . In our comparison of data and model we chose to keep the loop inductance fixed at its nominal design value because the lithographic process dictates the loop geometry to high precision. We adjusted the capacitance C and critical current $I_c(6.5 \text{ K})$ from their nominal design values to fit the experimentally observed resonant frequencies at $P = -80$ dBm using Eq. 2 and $P = -50$ dBm using Eq. 10 for $T = 6.5 \text{ K}$ and $\Phi_{DC} = 0$. The fit value for capacitance is 30% higher than the design value, which exceeds the 20% tolerance quoted for the Nb/ AlO_x /Nb process [71]. The sub-gap resistance $R = 820 \Omega$, and the filling fraction F and medium length l in Eqs. 13 and 14 were adjusted to match the width and depth of the observed $|S_{21}(\omega)|$ minimum at $\Phi_{DC} = 0$, $T = 6.5 \text{ K}$, and -80 dBm. With this set of parameters we are able to quantitatively explain the DC flux and rf power dependence of the RF SQUID meta-atom.

We were also able to extract the temperature dependence of the critical current $I_c(T)$ from the data for the flux dependence of the resonant frequency at different fixed temperatures. By noting the maximum resonant frequency as a function of flux we are able to deduce the critical current of the junction at each temperature using Eqs. 1 and 2. The results for $I_c(T)$, shown in Fig. 5, are consistent with previous results on Nb/ AlO_x /Al/Nb tunnel junctions [72].

The RF SQUID meta-atom proves to be remarkably tunable. We have demonstrated tunability with temperature, RF current, and DC magnetic flux. The temperature tunability has the unique feature that it can either increase or decrease the resonant frequency, depending on the DC magnetic flux applied to the meta-atom (rf power tunability has a similar dependence on dc flux).

The low-temperature resonant frequency is very sensitive to DC flux, and the slope of temperature (or rf flux) tuning of f_0 can be made large or small, and either positive or negative.

The RF current dependence of the SQUID meta-atom response is also quite unique. At low powers (< -70 dBm), and high powers (> -55 dBm), the meta-atom has a resonant interaction with electromagnetic radiation. However at intermediate RF powers the meta-atom becomes essentially transparent to electromagnetic radiation. This is similar to recent demonstrations of metamaterial-induced transparency in which a tunable “spectral hole” is created by interfering resonant processes in two or more meta-atoms making up a meta-molecule [73] [74] [75] [76]. There, the transparency condition in the superconducting meta-molecule could be suppressed in a switching transition at high power [39]. In our case, the transparency process is due to the non-linear Josephson effect and is self-induced, making transparency in the RF SQUID meta-atom much simpler than previous implementations. In addition the transparency condition arises from a decrease in dissipation without enhancement in loss at nearby frequencies, quite different from other realizations [77]. As such it is potentially very useful as a power limiter for sensitive front-end receivers [78], for example.

The DC flux tuning of the SQUID meta-atom is remarkably sensitive. At its maximum value, the flux tunability (defined as the frequency change divided by the change in magnetic field) is approximately 80 THz/Gauss, at 12 GHz and 6.5 K. Hence only extremely small magnetic fields are required to make very substantial changes in the properties of the meta-atom. The next question is how quickly this tuning can be achieved. Applying a localized magnetic field to the SQUID meta-atom can be accomplished with superconducting transmission lines carrying short pulses [65]. For example, tuning of SQUID-like superconducting qubits has been accomplished on nano-second time scales limited only by

the rise-time of the current pulse [79] [80].

Looking at the overall tunability of the meta-atom in normalized units, we have achieved a tunability (defined as tuning frequency range divided by the center frequency of tuning) of 56%. The meta-atom loss varies by about 64% (defined as the loss range divided by maximum loss) over this entire tuning range. We estimate the figure of merit (defined as the ratio of the real part of μ to the imaginary part) to be 1700 at the resonant frequency in the case of low power and zero DC flux. The goal of achieving wide meta-atom tunability on short time scales with low loss is well within reach. Future work will explore arrays of RF SQUID meta-atoms in both the interacting and non-interacting limits.

VII. CONCLUSION

We have designed, fabricated, and demonstrated an rf superconducting quantum interference device meta-atom in a geometry that can be scaled for free-space interactions with electromagnetic fields. The meta-atom proves to be highly tunable with dc magnetic field, rf currents, and temperature. The RF SQUID meta-atom proves to have low losses over its wide (56%) range of tunability. We have obtained a detailed quantitative understanding of this highly nonlinear meta-atom with first principles modeling of the element. The data and model are in excellent agreement. A novel form of electromagnetically-induced transparency has been observed in this meta-atom with increasing induced rf current.

ACKNOWLEDGMENTS

This work is supported by the NSF-GOALI program through grant #ECCS-1158644, and the Center for Nanophysics and Advanced Materials (CNAM). We thank Masoud Radparvar, Georgy Prokopenko, Jen-Hao Yeh and Tamin Tai for experimental guidance and helpful suggestions. We also thank H. J. Paik and M. V. Moody for use of the pulsed tube refrigerator.

-
- [1] V. G. Veselago, “The electrodynamics of substances with simultaneously negative values of epsilon and mu,” *Sov. Phys. Usp.* **10**, 509–514 (1968).
 - [2] D. R. Smith, W. J. Padilla, D. C. Vier, S. C. Nemat-Nasser, and S. Schultz, “Composite medium with simultaneously negative permeability and permittivity,” *Phys. Rev. Lett.* **84**, 4184–4187 (2000).
 - [3] R. A. Shelby, D. R. Smith, and S. Schultz, “Experimental verification of a negative index of refraction,” *Science* **292**, 77–79 (2001).
 - [4] J. B. Pendry, “Negative refraction makes a perfect lens,” *Phys. Rev. Lett.* **85**, 3966–3969 (2000).
 - [5] Z. Jacob, L. V. Alekseyev, and E. Narimanov, “Optical hyperlens: Far-field imaging beyond the diffraction limit,” *Opt. Express* **14**, 8247–8256 (2006).
 - [6] A. Alu and N. Engheta, “Pairing an epsilon-negative slab with a mu-negative slab: Resonance, tunneling and transparency,” *IEEE Trans. Antennas Propag.* **51**, 2558–2571 (2003).
 - [7] D. Schurig, J. J. Mock, B. J. Justice, S. A. Cummer, J. B. Pendry, A. F. Starr, and D. R. Smith, “Metamaterial electromagnetic cloak at microwave frequencies,” *Science* **314**, 977–980 (2006).
 - [8] Ulf Leonhardt, “Optical conformal mapping,” *Science* **312**, 1777–1780 (2006).
 - [9] J. B. Pendry, D. Schurig, and D. R. Smith, “Controlling electromagnetic fields,” *Science* **312**, 1780–1782 (2006).
 - [10] N. I. Landy, S. Sajuyigbe, J. J. Mock, D. R. Smith, and W. J. Padilla, “Perfect metamaterial absorber,” *Phys. Rev. Lett.* **100**, 7402 (2008).

- [11] Zhaowei Liu, Nicholas Fang, Ta-Jen Yen, and Xiang Zhang, "Rapid growth of evanescent wave by a silver superlens," *Appl. Phys. Lett.* **83**, 5184–5186 (2003).
- [12] R Ruppin, "Surface polaritons of a left-handed medium," *Phys. Lett. A* **277**, 61–64 (2000).
- [13] R Ruppin, "Surface polaritons of a left-handed material slab," *J. Phys.: Condens. Matter* **13**, 1811–1819 (2001).
- [14] F. D. M. Haldane, "Electromagnetic surface modes at interfaces with negative refractive index make a 'not-quite-perfect' lens," (2002), arXiv:cond-mat/0206420.
- [15] D. R. Smith, D. Schurig, M. Rosenbluth, S. Schultz, S. A. Ramakrishna, and J. B. Pendry, "Limitations on sub-diffraction imaging with a negative refractive index slab," *Appl. Phys. Lett.* **82**, 1506–1508 (2003).
- [16] T. Koschny, R. Moussa, and C. M. Soukoulis, "Limits on the amplification of evanescent waves of left-handed materials," *J. Opt. Soc. Am. B* **23**, 485–489 (2006).
- [17] John Dimmock, "Losses in left-handed materials," *Opt. Express* **11**, 2397–2402 (2003).
- [18] J. Zhou, T. Koschny, M. Kafesaki, E. N. Economou, J. B. Pendry, and C. M. Soukoulis, "Saturation of the magnetic response of split-ring resonators at optical frequencies," *Phys. Rev. Lett.* **95**, 223902 (2005).
- [19] Atsushi Ishikawa, Takuo Tanaka, and Satoshi Kawata, "Negative magnetic permeability in the visible light region," *Phys. Rev. Lett.* **95**, 237401 (2005).
- [20] Yaroslav A. Urzhumov and Gennady Shvets, "Optical magnetism and negative refraction in plasmonic metamaterials," *Solid State Commun.* **146**, 208–220 (2008).
- [21] R. W. Ziolkowski and A. D. Kipple, "Application of double negative materials to increase the power radiated by electrically small antennas," *IEEE Trans. Antennas Propag.* **51**, 2626–2640 (2003).
- [22] R. W. Ziolkowski and A. Erentok, "Metamaterial-based efficient electrically small antennas," *IEEE Trans. Antennas Propag.* **54**, 2113–2130 (2006).
- [23] A. A. Zharov, I. V. Shadrivov, and Y. S. Kivshar, "Nonlinear properties of left-handed metamaterials," *Phys. Rev. Lett.* **91** (2003).
- [24] E. B. Wikborg, V. K. Semenov, and K. K. Likharev, "RSFQ front-end for a software radio receiver," *IEEE Trans. Appl. Supercond.* **9**, 3615–3618 (1999).
- [25] D. K. Brock, O. A. Mukhanov, and J. Rosa, "Superconductor digital rf development for software radio," *IEEE Communications Mag.* **39**, 174–179 (2001); O. A. Mukhanov, D. Kirichenko, I. V. Vernik, T. V. Filippov, A. Kirichenko, V. Dotsenko R. Webber, A. Talalaevskii, J. C. Tang, A. Sahu, P. Shevchenko, R. Miller, S. B. Kaplan, S. Sarwana, and D. Gupta, "Superconductor digital-rf receiver systems," *IEICE Trans. Electron.* **E91-C**, 306–317 (2008).
- [26] Steven M. Anlage, "The physics and applications of superconducting metamaterials," *J. Opt.* **13**, 024001 (2011).
- [27] J. Gittleman, B. Rosenblum, T. E. Seidel, and A. W. Wicklund, "Nonlinear reactance of superconducting films," *Physical Review* **137**, A527–A536 (1965).
- [28] S. K. Yip and J. A. Sauls, "Nonlinear meissner effect in CuO superconductors," *Phys. Rev. Lett.* **69**, 2264–2267 (1992).
- [29] M. Tinkham, *Introduction to Superconductivity*, 2nd ed. (McGraw-Hill, New York, 1996).
- [30] E. N. Economou, "Surface plasmons in thin films," *Phys. Rev.* **182**, 539–554 (1969).
- [31] T. B. Samoiloova, "Nonlinear microwave effects in thin superconducting films," *Supercond. Sci. Technol.* **8**, 259–278 (1995).
- [32] Matthias Hein, *High-temperature-superconductor thin films at microwave frequencies* (Springer-Verlag, Berlin, 1999).
- [33] M. Ricci, N. Orloff, and S. M. Anlage, "Superconducting metamaterials," *Appl. Phys. Lett.* **87**, 034102 (2005).
- [34] M. C. Ricci and S. M. Anlage, "Single superconducting split-ring resonator electrostatics," *Appl. Phys. Lett.* **88**, 264102 (2006).
- [35] J. Q. Gu, R. Singh, Z. Tian, W. Cao, Q. R. Xing, M. X. He, J. W. Zhang, J. G. Han, H. T. Chen, and W. L. Zhang, "Terahertz superconductor metamaterial," *Appl. Phys. Lett.* **97** (2010).
- [36] V. A. Fedotov, A. Tsiatmas, J. H. Shi, R. Buckingham, P. de Groot, Y. Chen, S. Wang, and N. I. Zheludev, "Temperature control of fano resonances and transmission in superconducting metamaterials," *Opt. Express* **18**, 9015–9019 (2010).
- [37] Hou-Tong Chen, Hao Yang, Ranjan Singh, John F. O'Hara, Abul K. Azad, Stuart A. Trugman, Q. X. Jia, and Antoinette J. Taylor, "Tuning the resonance in high-temperature superconducting terahertz metamaterials," *Phys. Rev. Lett.* **105**, 247402 (2010).
- [38] Jingbo Wu, Biaobing Jin, Yuhua Xue, Caihong Zhang, Hao Dai, Labao Zhang, Chunhai Cao, Lin Kang, Weiwei Xu, Jian Chen, and Peiheng Wu, "Tuning of superconducting niobium nitride terahertz metamaterials," *Opt. Express* **19**, 12021–12026 (2011).
- [39] Cihan Kurter, Philippe Tassin, Alexander P. Zhuravel, Lei Zhang, Thomas Koschny, Alexey V. Ustinov, Costas M. Soukoulis, and Steven M. Anlage, "Switching nonlinearity in a superconductor-enhanced metamaterial," *Appl. Phys. Lett.* **100**, 121906–3 (2012).
- [40] V. Savinov, V. A. Fedotov, S. M. Anlage, P. A. J. de Groot, and N. I. Zheludev, "Modulating sub-THz radiation with current in superconducting metamaterial," *Phys. Rev. Lett.* **109**, 243904 (2012).
- [41] S. M. Anlage, H. J. Snortland, and M. R. Beasley, "A current controlled variable delay superconducting transmission-line," *IEEE Trans. Magn.* **25**, 1388–1391 (1989).
- [42] S. Tahara, S. M. Anlage, J. Halbritter, C. B. Eom, D. K. Fork, T. H. Geballe, and M. R. Beasley, "Critical currents, pinning, and edge barriers in narrow YBa₂Cu₃O_{7- δ} thin-films," *Phys. Rev. B* **41**, 11203–11208 (1990).
- [43] M. C. Ricci, H. Xu, R. Prozorov, A. P. Zhuravel, A. V. Ustinov, and S. M. Anlage, "Tunability of superconducting metamaterials," *IEEE Trans. Appl. Supercond.* **17**, 918–921 (2007).
- [44] Biaobing Jin, Caihong Zhang, Sebastian Engelbrecht, Andrei Pimenov, Jingbo Wu, Qinyin Xu, Chunhai Cao, Jian Chen, Weiwei Xu, Lin Kang, and Peiheng Wu, "Low loss and magnetic field-tunable superconducting terahertz metamaterial," *Opt. Express* **18**, 17504–17509 (2010).
- [45] A. P. Zhuravel, S. M. Anlage, and A. V. Ustinov, "Microwave current imaging in passive HTS components by low-temperature laser scanning microscopy (LTLSM)," *J. Supercond. Novel Magn.* **19**, 625–632 (2006).
- [46] A. P. Zhuravel, A. G. Sivakov, O. G. Turutanov, A. N. Omelyanchouk, S. M. Anlage, A. Lukashenko, A. V.

- Ustinov, and D. Abrahimov, "Laser scanning microscopy of HTS films and devices (review article)," *Low Temp. Phys.* **32**, 592–607 (2006).
- [47] C. Kurter, A. P. Zhuravel, J. Abrahams, C. L. Bennett, A. V. Ustinov, and S. M. Anlage, "Superconducting rf metamaterials made with magnetically active planar spirals," *IEEE Trans. Appl. Supercond.* **21**, 709–712 (2011).
- [48] Cihan Kurter, Alexey V. Zhuravel, Alexander P. Ustinov, and Steven M. Anlage, "Microscopic examination of hot spots giving rise to nonlinearity in superconducting resonators," *Phys. Rev. B* **84**, 104515 (2011).
- [49] Alexander P. Zhuravel, Cihan Kurter, Alexey V. Ustinov, and Steven M. Anlage, "Unconventional rf photoresponse from a superconducting spiral resonator," *Phys. Rev. B* **85**, 134535 (2012).
- [50] V. Savinov, A. Tsiatmas, A. R. Buckingham, V. A. Fedotov, P. A. de Groot, and N. I. Zheludev, "Flux exclusion superconducting quantum metamaterial: Towards quantum-level switching," *Sci. Rep.* **2**, 450 (2012).
- [51] T. P. Orlando and K. A. Delin, *Foundations of Applied Superconductivity* (Addison-Wesley, Reading, MA, 1991).
- [52] K. K. Likharev, *Dynamics of Josephson Junctions and Circuits* (Gordon and Breach, New York, 1986).
- [53] F. Auracher and T. Van Duzer, "Rf impedance of superconducting weak links," *J. Appl. Phys.* **44**, 848–851 (1973).
- [54] H. Salehi, A. H. Majedi, and R. R. Mansour, "Analysis and design of superconducting left-handed transmission lines," *IEEE Trans. Appl. Supercond.* **15**, 996–999 (2005).
- [55] H. Salehi, R. R. Mansour, and A. H. Majedi, "Nonlinear Josephson left-handed transmission lines," *IET Microw. Antennas Propag.* **1**, 69–72 (2007).
- [56] A. H. Silver and J. E. Zimmerman, "Quantum states and transitions in weakly connected superconducting rings," *Phys. Rev.* **157**, 317 (1967), pR.
- [57] B. Chesca, M. Muck, and Y. Zhang, *Radio Frequency SQUIDS and Their Applications*, Microwave Superconductivity (Kluwer Academic Publishers, Dordrecht, 2001).
- [58] C. G. Du, H. Y. Chen, and S. Q. Li, "Quantum left-handed metamaterial from superconducting quantum-interference devices," *Phys. Rev. B* **74**, 113105 (2006).
- [59] C. G. Du, H. Y. Chen, and S. Q. Li, "Stable and bistable SQUID metamaterials," *J. Phys.: Condens. Matter* **20**, 345220 (2008).
- [60] N. Lazarides and G. P. Tsironis, "Rf superconducting quantum interference device metamaterials," *Appl. Phys. Lett.* **90**, 163501 (2007).
- [61] A. I. Maimistov and I. R. Gabitov, "Nonlinear response of a thin metamaterial film containing Josephson junctions," *Opt. Commun.* **283**, 1633–1639 (2010).
- [62] A. L. Rakhmanov, A. M. Zagoskin, S. Savel'ev, and F. Nori, "Quantum metamaterials: Electromagnetic waves in a Josephson qubit line," *Phys. Rev. B* **77**, 144507 (2008).
- [63] M. A. Castellanos-Beltran and K. W. Lehnert, "Widely tunable parametric amplifier based on a superconducting quantum interference device array resonator," *Appl. Phys. Lett.* **91**, 083509 (2007).
- [64] M. A. Castellanos-Beltran, K. D. Irwin, G. C. Hilton, L. R. Vale, and K. W. Lehnert, "Amplification and squeezing of quantum noise with a tunable Josephson metamaterial," *Nature Phys.* **4**, 928–931 (2008).
- [65] P. Jung, S. Butz, S. V. Shitov, and A. V. Ustinov, "Low-loss tunable metamaterials using superconducting circuits with Josephson junctions," *Appl. Phys. Lett.* **102**, 062601–4 (2013), arXiv:1204.7371, arXiv: 1305.2910.
- [66] Charles M. Falco, "Phase-space of a driven, damped pendulum (Josephson weak link)," *Am. J. Phys.* **44**, 733 (1976).
- [67] B. Chesca, "Theory of rf squids operating in the presence of large thermal fluctuations," *J. Low Temp. Phys.* **110**, 963–1001 (1998).
- [68] Stuart Bermon and Tushar Gheewala, "Moat-guarded Josephson SQUIDS," *IEEE Trans. Magn.* **19**, 1160–1164 (1983).
- [69] Whiteley Research Inc., <http://www.wrcad.com/> (2004).
- [70] David R. Smith and John B. Pendry, "Homogenization of metamaterials by field averaging," *J. Opt. Soc. Am. B* **23**, 391–403 (2006).
- [71] Hypres, "Niobium integrate circuit fabrication process #03-10-45 design rules," <http://www.hypres.com/foundry/niobium-process/> (2008).
- [72] I.P. Nevirkovets, J. B. Ketterson, and J. M. Rowell, "Modified superconductor-insulator-normal metal-insulator-superconductor Josephson junctions with high critical parameters," *J. Appl. Phys.* **89**, 3980–3985 (2001).
- [73] V. A. Fedotov, M. Rose, S. L. Prosvirnin, N. Papasimakis, and N. I. Zheludev, "Sharp trapped-mode resonances in planar metamaterials with a broken structural symmetry," *Phys. Rev. Lett.* **99**, 147401 (2007).
- [74] N. Papasimakis, V. A. Fedotov, N. I. Zheludev, and S. L. Prosvirnin, "Metamaterial analog of electromagnetically induced transparency," *Phys. Rev. Lett.* **101**, 253903 (2008).
- [75] P. Tassin, Lei Zhang, Th. Koschny, E. N. Economou, and C. M. Soukoulis, "Low-loss metamaterials based on classical electromagnetically induced transparency," *Phys. Rev. Lett.* **102**, 053901 (2009).
- [76] Cihan Kurter, Philippe Tassin, Lei Zhang, Thomas Koschny, Alexander P. Zhuravel, Alexey V. Ustinov, Steven M. Anlage, and Costas M. Soukoulis, "Classical analogue of electromagnetically induced transparency with a metal-superconductor hybrid metamaterial," *Phys. Rev. Lett.* **107**, 043901 (2011).
- [77] A. A. Abdumalikov, O. Astafiev, A. M. Zagoskin, Y. A. Pashkin, Y. Nakamura, and J. S. Tsai, "Electromagnetically induced transparency on a single artificial atom," *Phys. Rev. Lett.* **104**, 3601 (2010).
- [78] O. Mukhanov, D. Gupta, A. Kadin, and V. Semenov, "Superconductor analog-to-digital converters," *Proc. of the IEEE* **92**, 1564–1584 (2004).
- [79] F. G. Paauw, A. Fedorov, C. J. P. M Harmans, and J. E. Mooij, "Tuning the gap of a superconducting flux qubit," *Phys. Rev. Lett.* **102**, 090501 (2009).
- [80] Xiaobo Zhu, Alexander Kempand Shiro Saito, and Kouichi Semba, "Coherent operation of a gap-tunable flux qubit," *Appl. Phys. Lett.* **97**, 102503 (2010).